Navier-Stokes Simulation of UH-60A Rotor/Wake Interaction Using Adaptive Mesh Refinement

Neal M. Chaderjian
NASA Ames Research Center
Moffett Field, CA 94035

Blackhawk Helicopter Flying Over NASA Ames Research Center

Presented at the
AHS International 73rd Annual Forum
Fort Worth, TX, USA
May 9-11, 2017

Motivation

- Average CFD FM accuracy was 2.4% (2009)
  - ❖ It was believed that poor rotor wake resolution was responsible
  - ❖ This lead to research in off-body (OB) adaptive mesh refinement (AMR)
- In 2011 (Chaderjian/Buning): CFD FM predicted with 0.2% for V22 TRAM
  - ❖ Vortex wake resolution had no effect (10%, 5%, and 2.5% c_{tip})
  - ❖ Rather, it was crucial to
    - Adequately resolve the formation of the blade-tip vortex
      - ✧ Fine surface mesh near rotor tip and high-order spatial accuracy
    - Maintain a physically realistic turbulent eddy viscosity in the vortex wake
      - ✧ Detached eddy simulation (DES) turbulent length scale

Coarse Wake-Grid Resolution $\Delta S=10\%c_{tip}$

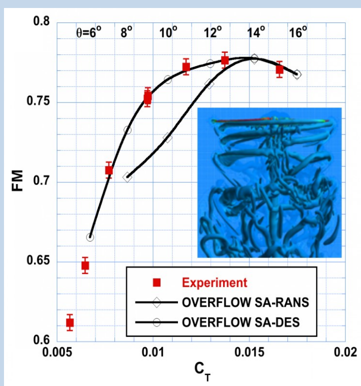

No Difference In the FM

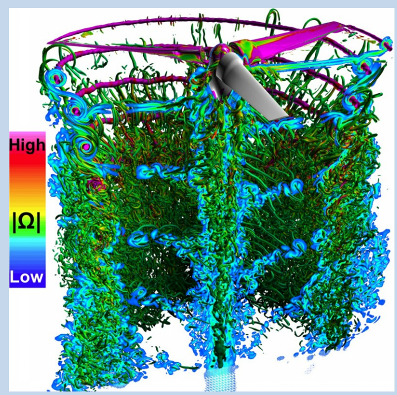

Fine Wake-Grid Resolution $\Delta S=2.5\%c_{tip}$

Motivation

- In 2012 (Chaderjian/Ahmad): UH-60A rotor in hover and forward flight (C8534)
  - ❖ Airloads did not depend on rotor wake resolution
- **Both studies did not involve significant blade/wake interaction**

Coarse Wake-Grid
Resolution
ΔS=10%c_{tip}

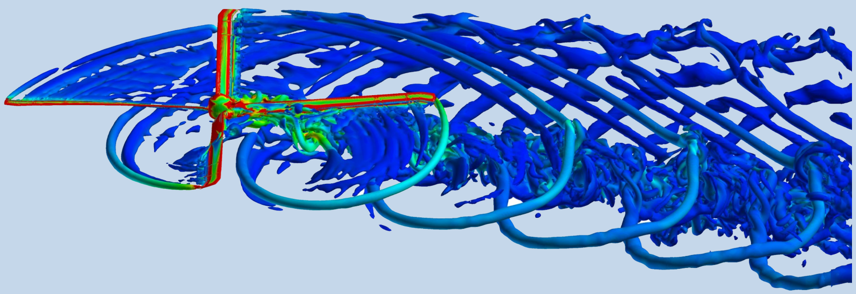

Fine Wake-Grid
Resolution
ΔS=2.5%c_{tip}

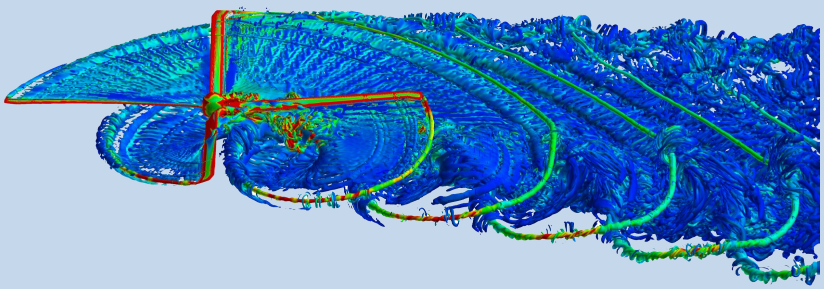

Objective

- **An important question remains**
  - How are the forward-flight CFD airloads affected by rotor-wake resolution when there is significant blade/wake interaction?
  - Practical engineering issue: High resolution wakes are too expensive for most engineering applications
- Two examples for a UH-60A rotor in forward flight are examined
  - Blade vortex interaction (BVI), flight-test counter C8513
  - Dynamic stall with BVI, flight-test counter C9017
- Also examine 2D dynamic stall
  - Discuss similarities and differences in 2D and 3D dynamic stall

Outline

- Flight-Test Data
- Numerical Approach
- Numerical Results
    - BVI – UH-60A (C8513)
    - Dynamic stall
        - 2D example
        - 3D UH-60A (C9017)
- Concluding Remarks

Flight-Test Data/CFD Validation

- Joint NASA/U.S. Army UH-60A Airloads Database (1993/1994)
  - ❖ Airloads at various radial locations along the rotor blade
- Bousman's qualitative analysis of dynamic stall (AHS Journal/Oct. 1998)
  - ❖ He examined the time history of blade pressures to judge when
    - Moment stall: Formation of dynamic stall vortex at blade leading edge
    - Lift stall: When dynamic stall vortex passes over blade trailing edge
    - Flow separation at blade trailing edge

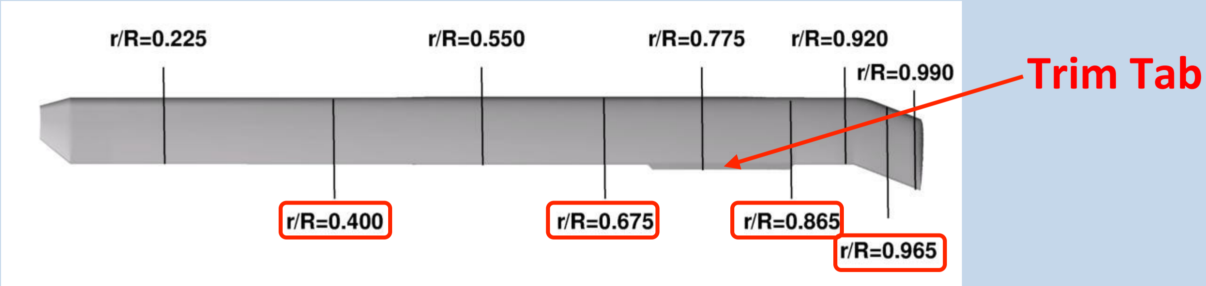

Numerical Approach
(CFD/CSD Loose Coupling)

Loose
Coupling
Every
¼ revolution

OVERFLOW 2.2L – CFD Flow Solver

- Solves the time-dependent Navier-Stokes equations
  - ❖ Structured overset grids
  - ❖ **2^{nd}-order** dual time accuracy (Δt=¼° rotation, 60 subiterations)
    - ▪ At least 2.3 subiteration residual drop for all grids
  - ❖ **5^{th}-order** spatial accuracy (central differences/artificial dissipation)
  - ❖ **Hybrid RANS/LES** turbulence model
    - ▪ Spalart-Allmaras one-equation turbulence model
    - ▪ DDES length scale
    - ▪ SARC rotation/curvature correction
    - ▪ Y^+<1 at body surfaces

CAMRAD II – Helicopter Comprehensive Analysis Code

- Provides rotor-blade structural deflections
- Provides trim control angles at the blade root

Numerical Approach

(Near-Body and Off-Body Grids)

Cartesian Off-Body Grids

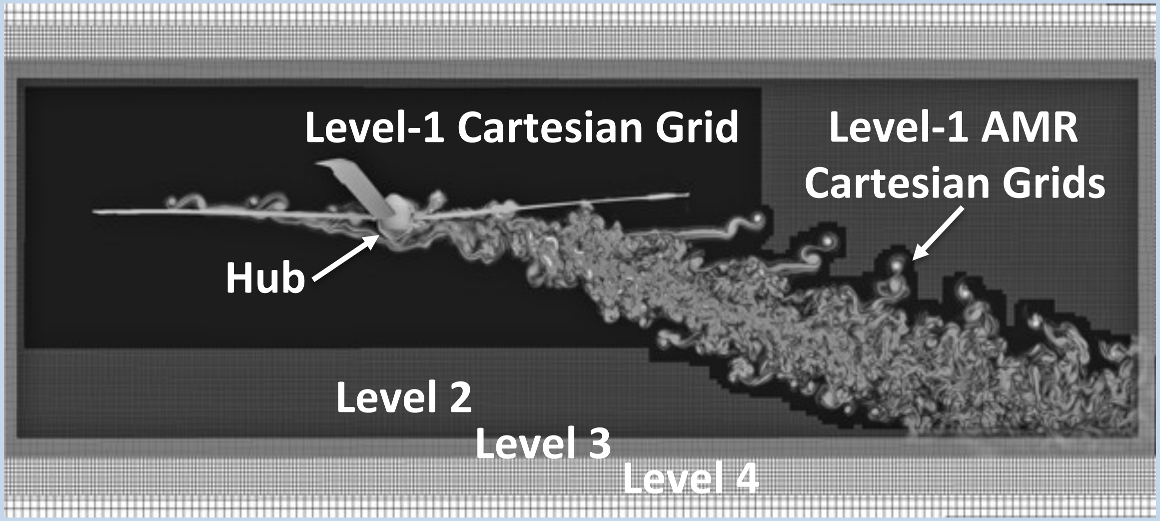

Rotor-Blade Grids

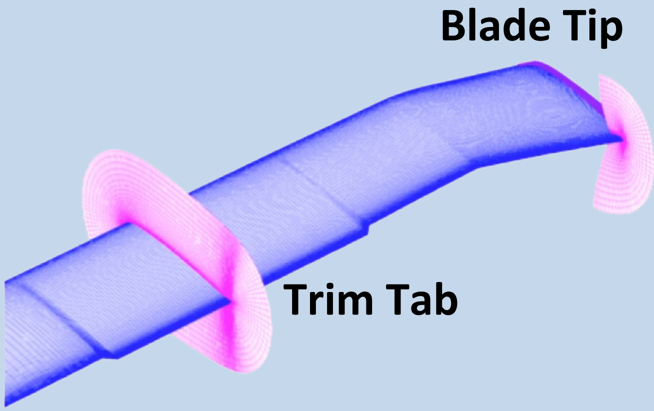

- Rotor blades/Hub use O-mesh topology
- Off-body grids use Cartesian grids with adaptive mesh refinement (AMR)
- Rotor wake captured **only with** Level-1 grids (10%, 5%, and 2.5%c_{tip})
- No interpolation throughout the resolved rotor wake of interest
  - ❖ Has same resolution and coincident overlaping grid points

Outline

- Flight-Test Data
- Numerical Approach
- Numerical Results
    - **BVI – UH-60A (C8513)**
    - Dynamic stall
        - 2D example
        - 3D UH-60A (C9017)
- Concluding Remarks

BVI Flight Counter C8534
NASA'S OVERFLOW Navier-Stokes CFD Code

M_∞	M_{tip}	μ	Re_{tip}	α_{shaft}, deg	β, deg	C_T
0.0982	0.643	0.153	7.15×10^6	0.75	7.71	0.00675

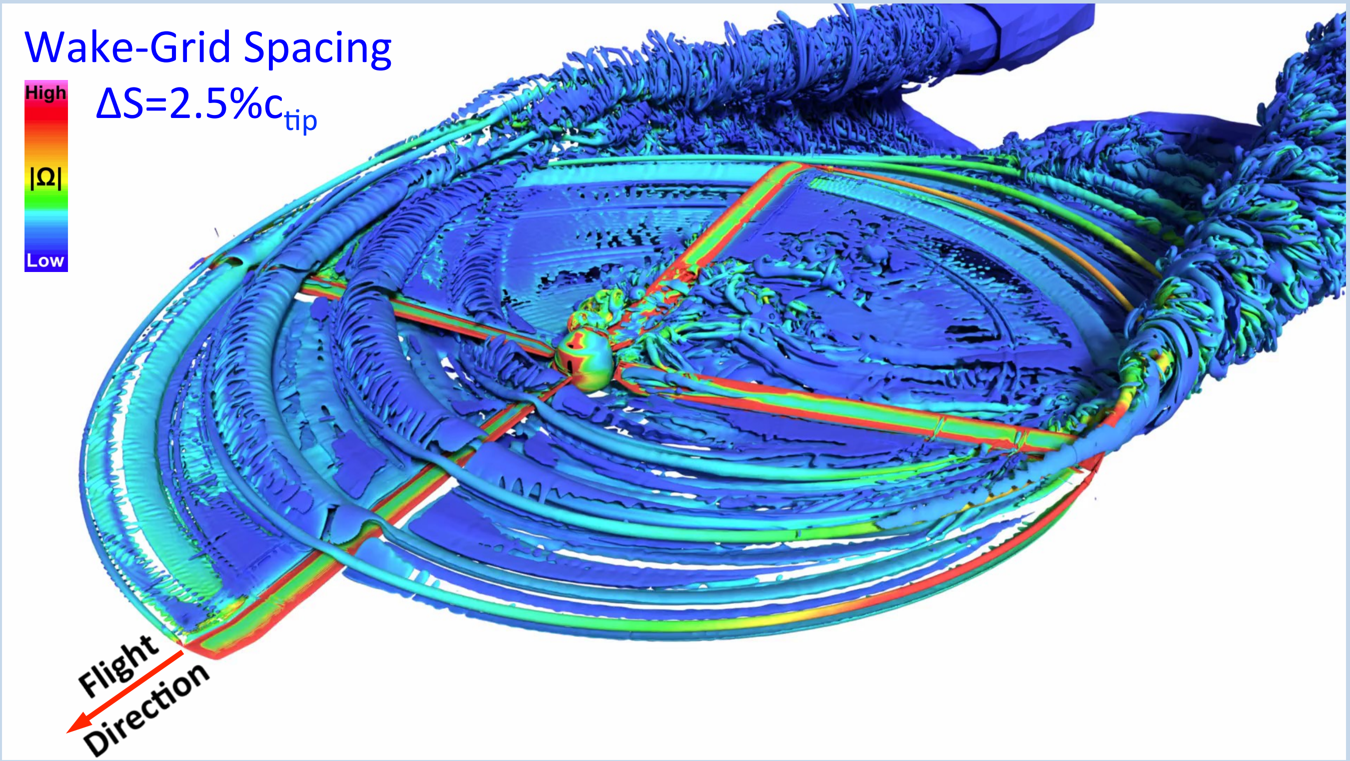

Three AMR Wake-Grid Resolutions

BVI Flight Counter C8534

NASA's Pleiades Supercomputer

5,628 Broadwell CPU Cores

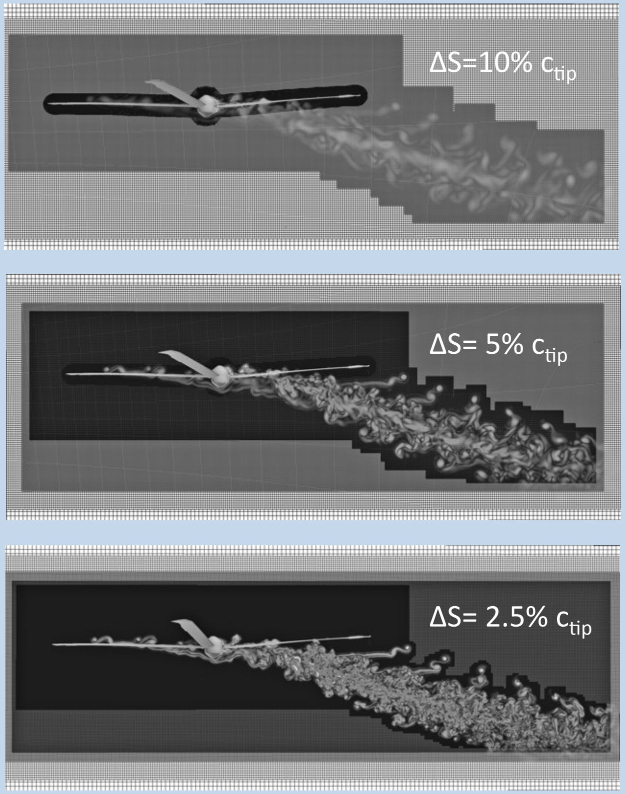

500 Grids
87 Million Grid Points
4.6 Hr/Rev

2,500 Grids
297 Million Grid Points
7.8 Hr/Rev

12,000 Grids
1.8 Billion Grid Points
40 Hr/Rev

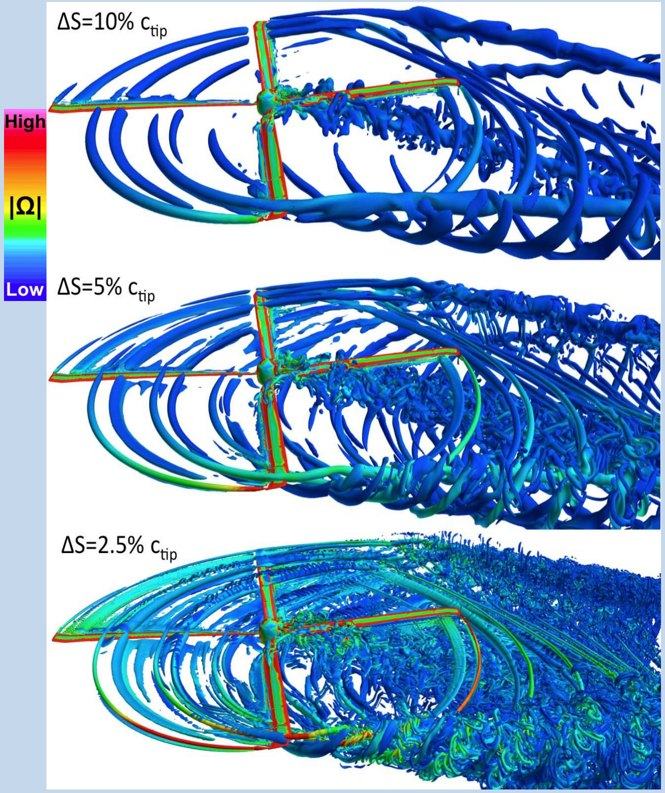

Effect of Wake-Grid Resolution on Airloads

BVI Flight Counter C8534

- Good overall agreement with flight-test data
- OB resolution has very little effect on airloads!

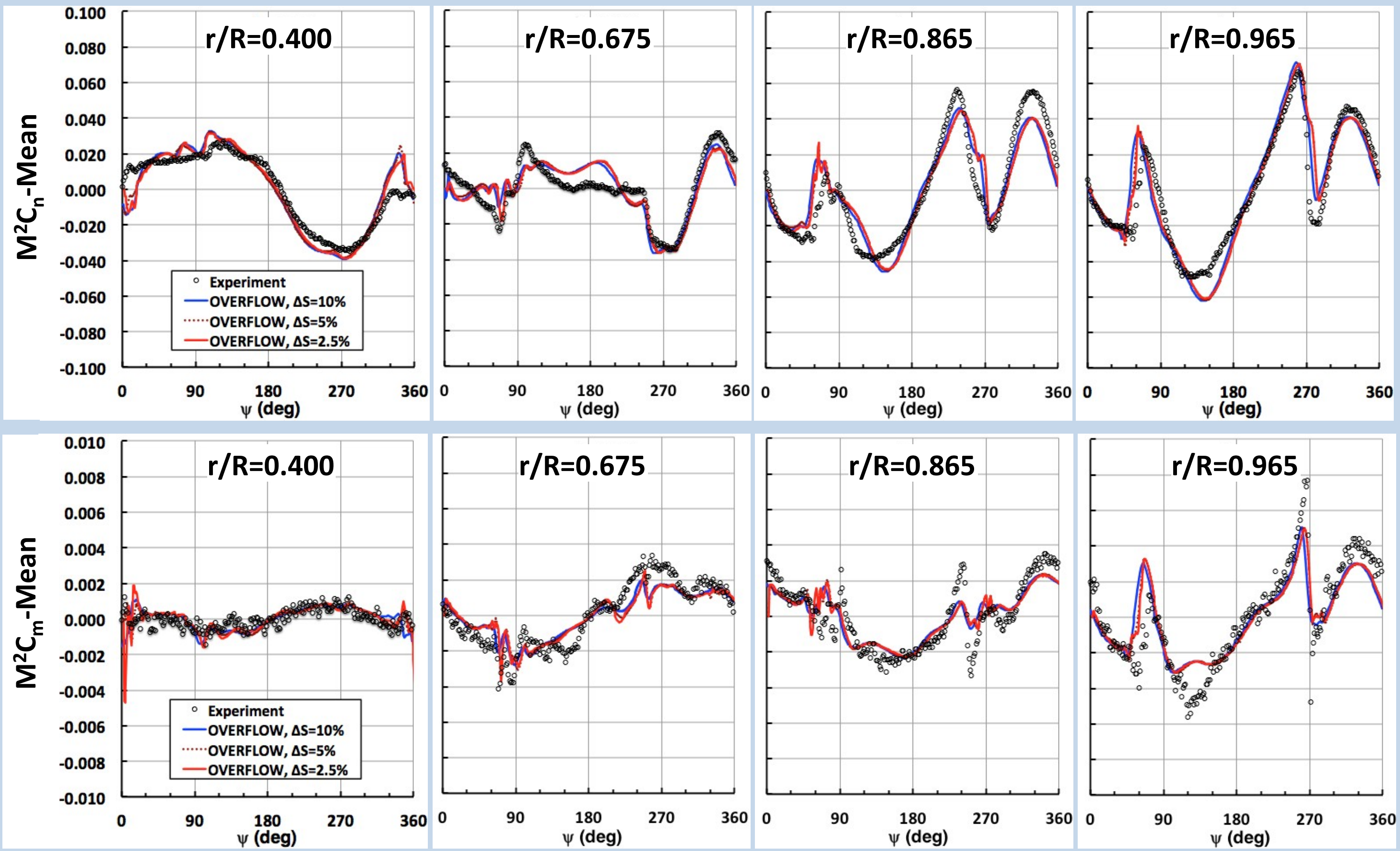

Outline

- Flight-Test Data
- Numerical Approach
- Numerical Results
  - BVI – UH-60A (C8513)
  - **Dynamic stall**
    - **2D example**
    - 3D UH-60A (C9017)
- Concluding Remarks

CFD Animation of Two-Dimensional Dynamic Stall

$$\alpha = 10^\circ + 10^\circ \sin(2kt - \tfrac{\pi}{2}),\ k = \frac{\omega c}{2V_\infty} = 0.1$$

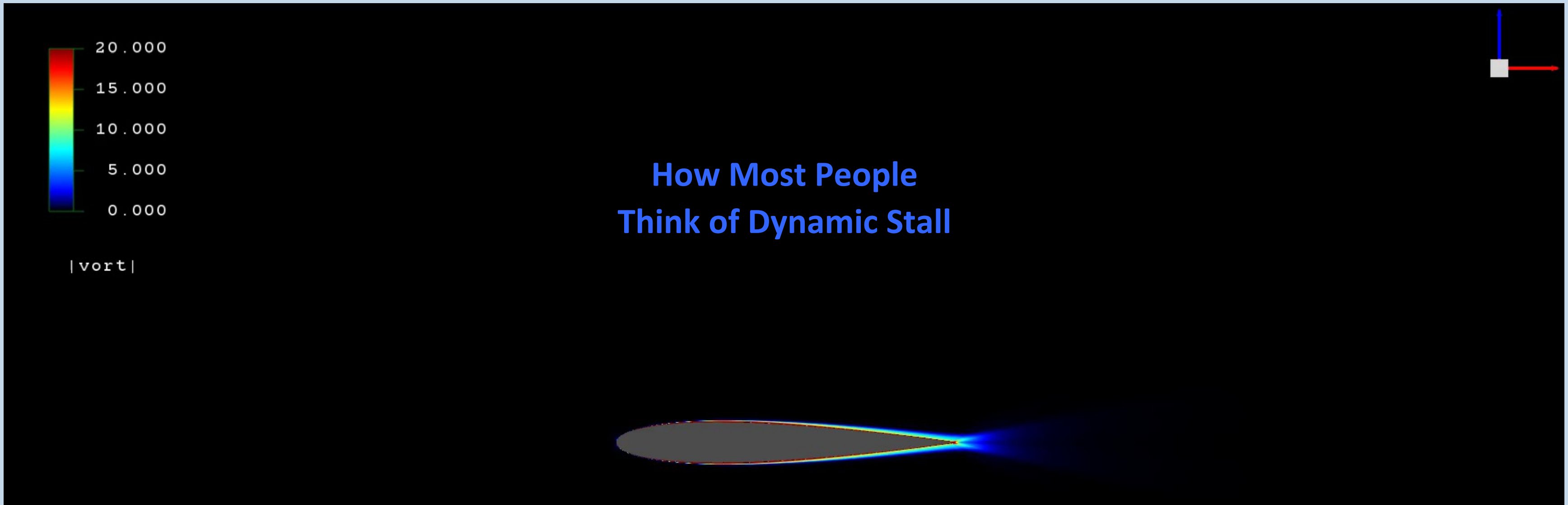

- Vortex forming at airfoil leading edge – (moment stall)
- Vortex passing airfoil trailing edge – (lift stall)
- Reversed flow
  - As vortex forms at leading edge
  - As vortex passes trailing edge
- Three stall events, each smaller than the previous one

Two-Dimensional Dynamic Stall

$$\alpha = 10^\circ + 10^\circ \sin(2kt - \tfrac{\pi}{2}),\ k = \frac{\omega c}{2V_\infty} = 0.1$$

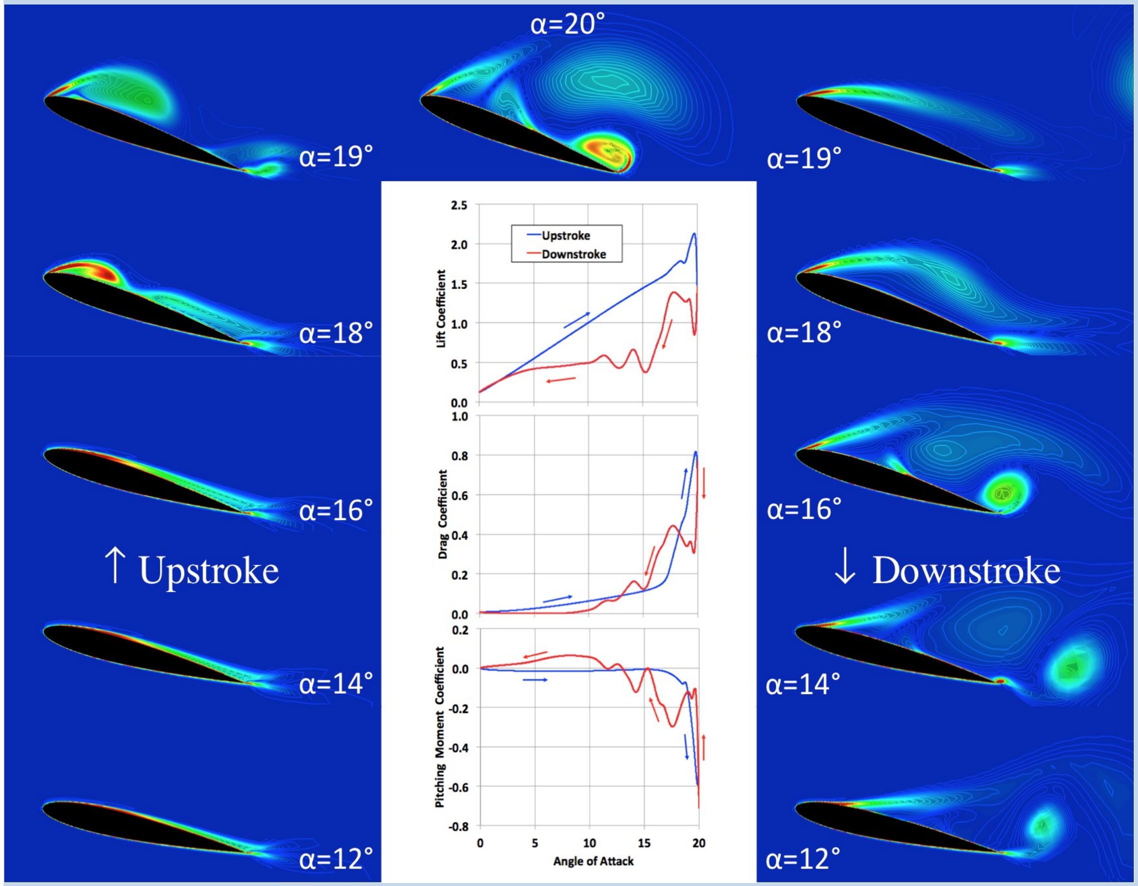

- Force/moment time-history indicates 3 stall events
  - ❖ 2-3 typical
  - ❖ 2D characteristics identified experimentally (McCroskey et al., 1976)
  - ❖ Many feel 2D captures the essential elements (Tan & Carr, 1996)
  - ❖ It will be shown that 2D does miss some important 3D dynamic stall characteristics

Outline

- Flight-Test Data
- Numerical Approach
- Numerical Results
  - BVI – UH-60A (C8513)
  - **Dynamic stall**
    - 2D example
    - **3D UH-60A (C9017)**
- Concluding Remarks

High-Resolution Dynamic Stall (C9017)
NASA'S OVERFLOW Navier-Stokes CFD Code

RVLT

M_∞	M_{tip}	μ	Re_{tip}	α_{shaft}, deg	β, deg	C_T
0.158	0.666	0.237	4.62×10^6	-0.15	-1.58	0.0110

There is BVI

It is affecting the dynamic stall process

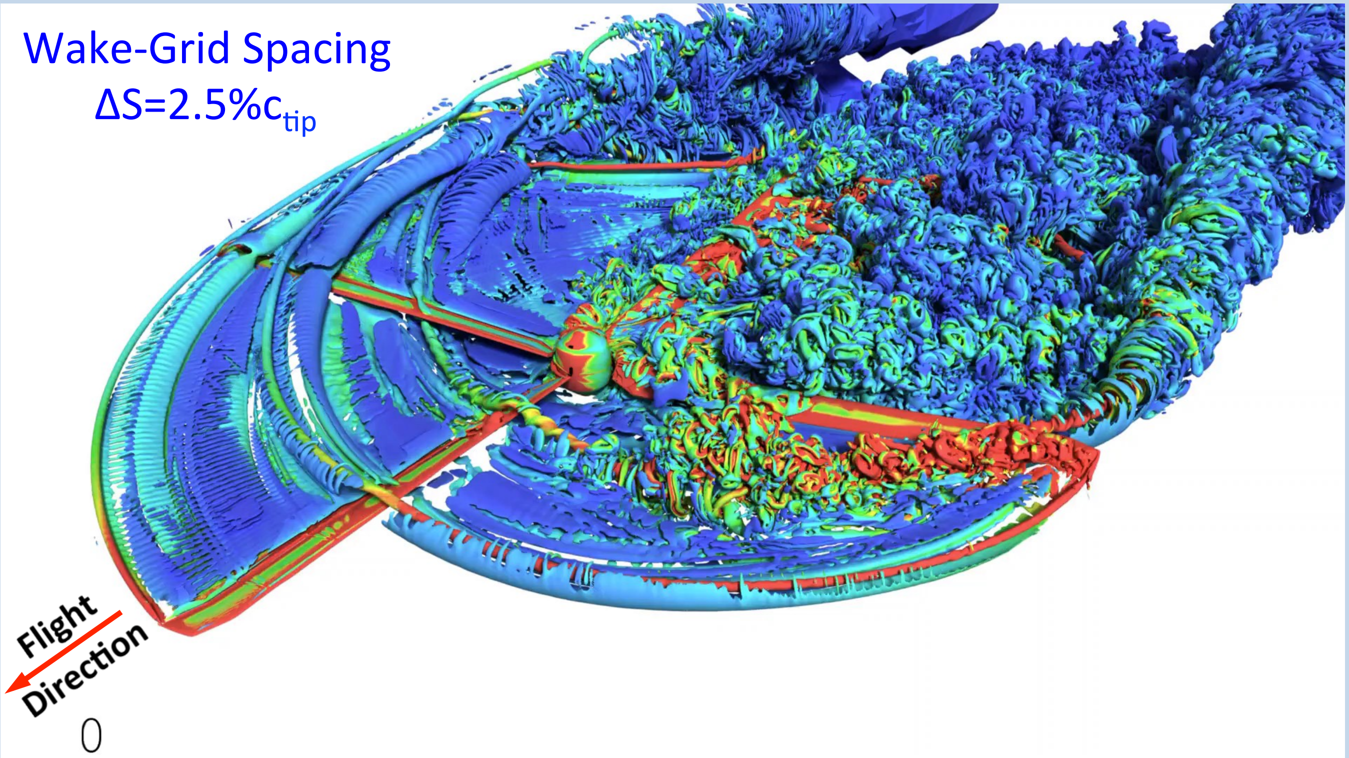

Three AMR Wake-Grid Resolutions

BVI Flight Counter C8534

NASA's Pleiades Supercomputer

5,628 Broadwell CPU Cores

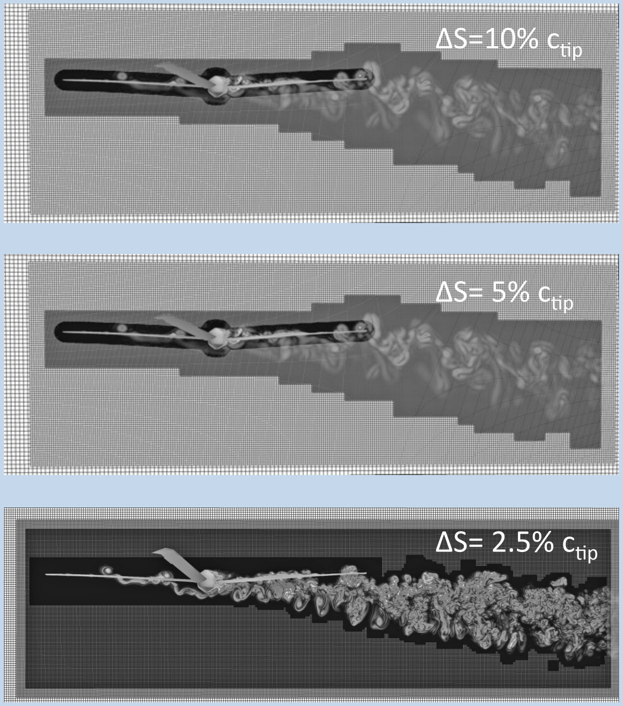

760 Grids
83 Million Grid Points
4.5 Hr/Rev

3,200 Grids
241 Million Grid Points
6.2 Hr/Rev

14,700 Grids
1.3 Billion Grid Points
28.5 Hr/Rev

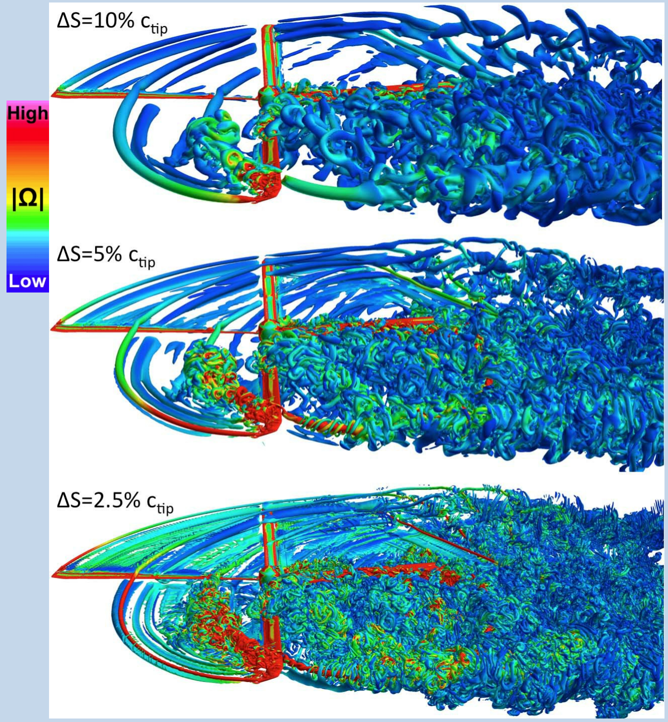

Effect of Wake-Grid Resolution on Airloads

Dynamic Stall Flight Counter C8534

- Good overall agreement with flight-test data
- More high-frequency content, but little effect on airloads!
- **This suggests $\Delta S=10\%c_{tip}$ adequate for engineering design airloads**

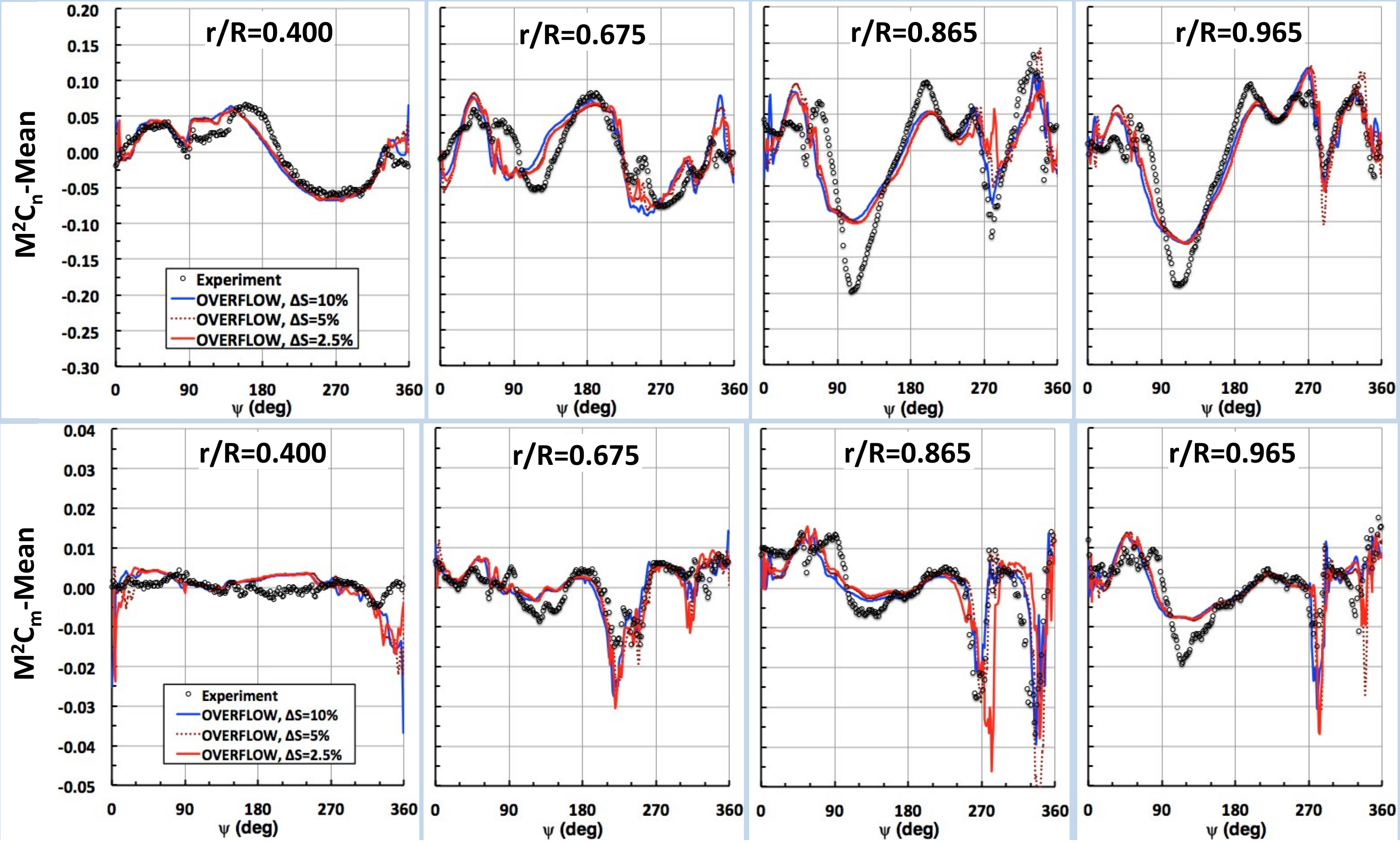

Closeup View of 3D Dynamic Stall With BVI

- Inboard and outboard separation, with attached flow in between
- 3D Vortex rings emitted due to Helmholtz vortex theorem
  - ❖ Different from 2D Vortex lift-off
- Vortex path altered due to separation
  - ❖ Can effect aeromechanics of following rotor blades

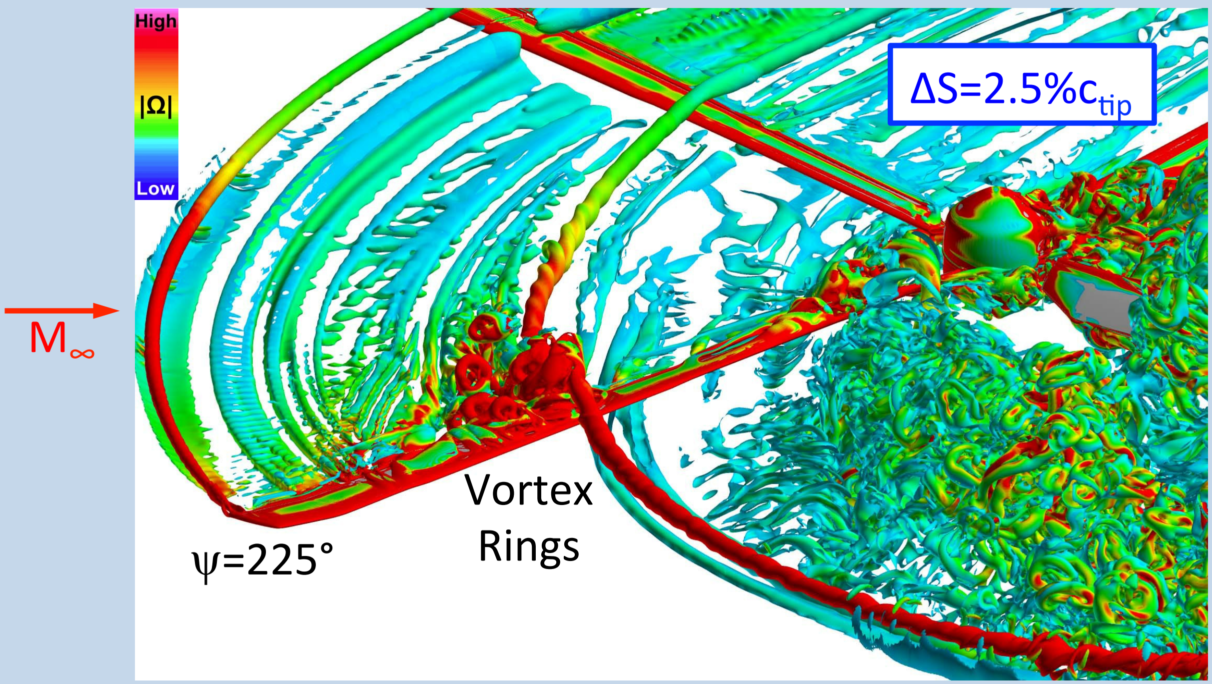

Closeup View of Dynamic Stall

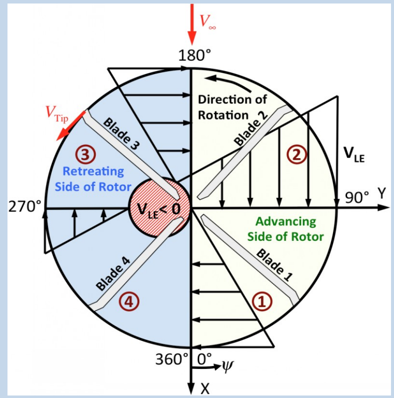

Nomenclature

- Flow separates outboard of vortex, remains attached inboard of vortex
- Separation moves with the vortices
- Tip vortices from Blades 2 and 3 appear to trigger dynamic stall

- Tip vortices from Blades 2 and 3 do not disrupt the flow on Blade 1

Blade 1 at ψ=180°

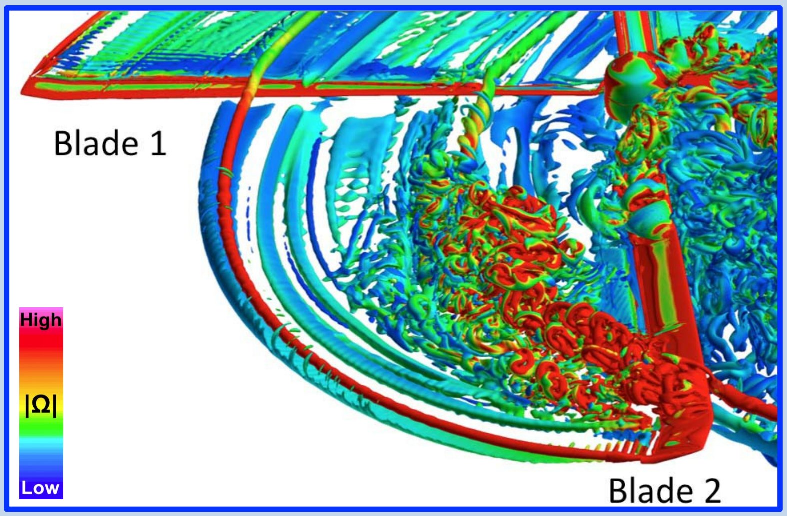

ΔS=2.5%c_{tip}

Blade 1 at ψ=225°

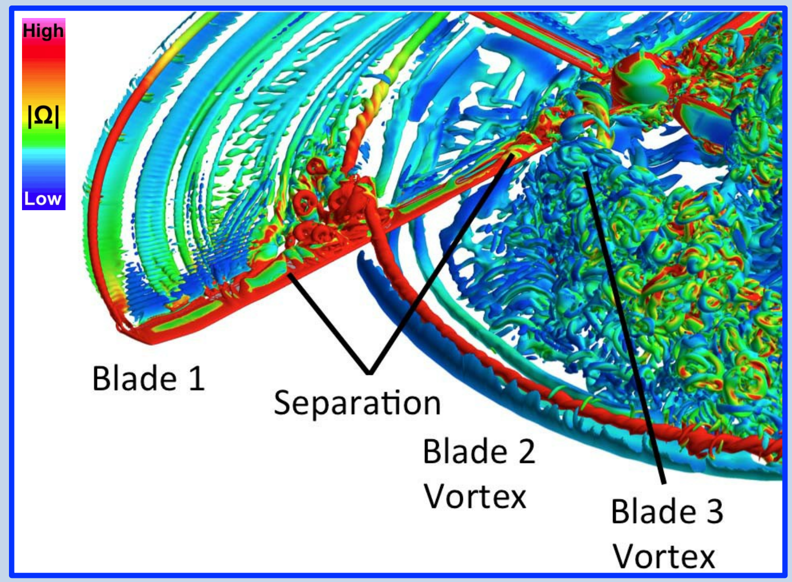

Rotating Blackhawk Rotor Blade

But What Happens When a Vortex Passes Over the Blade?

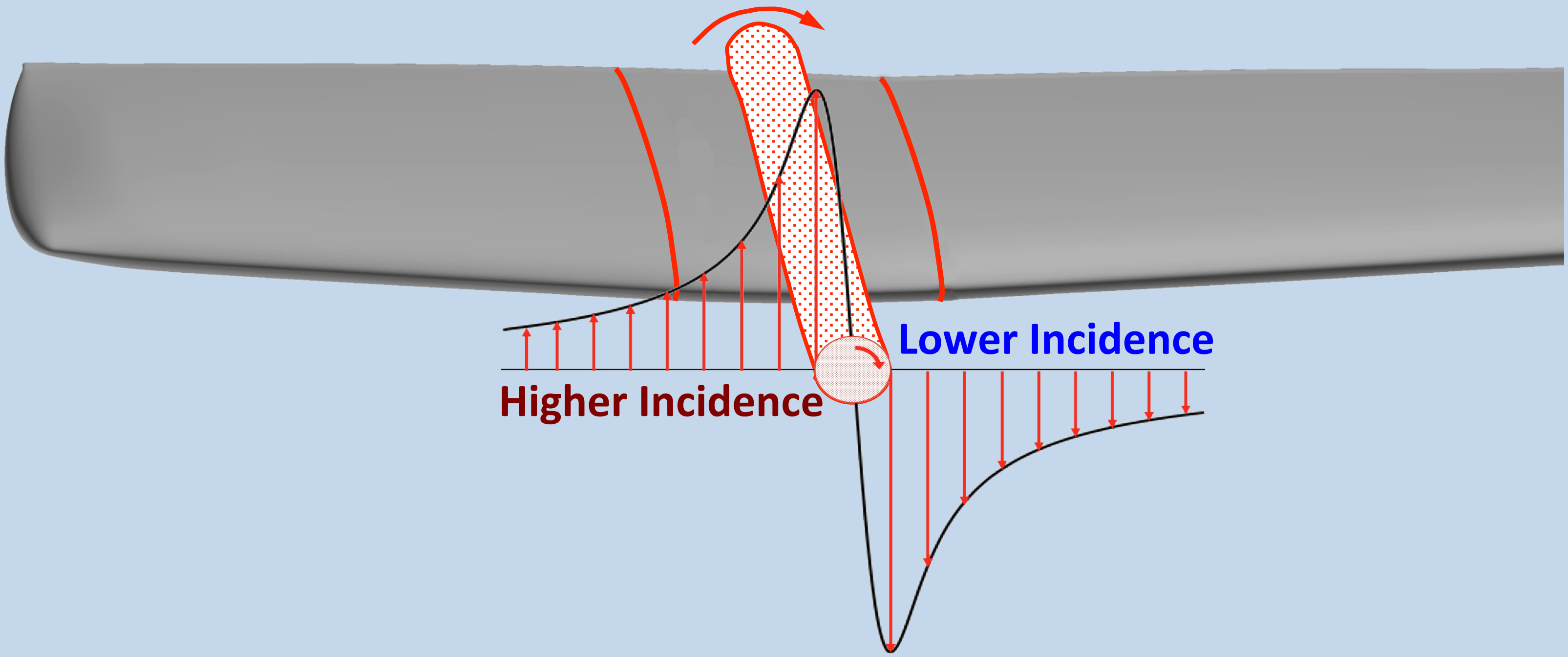

Velocity Vectors Relative to Rotor Blade

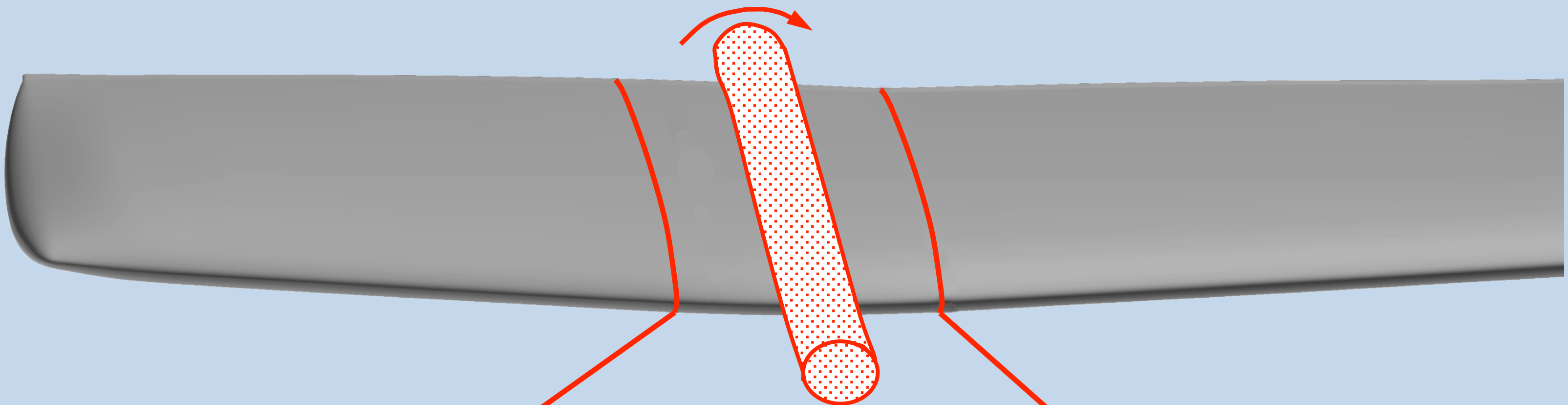

Outboard of Vortex

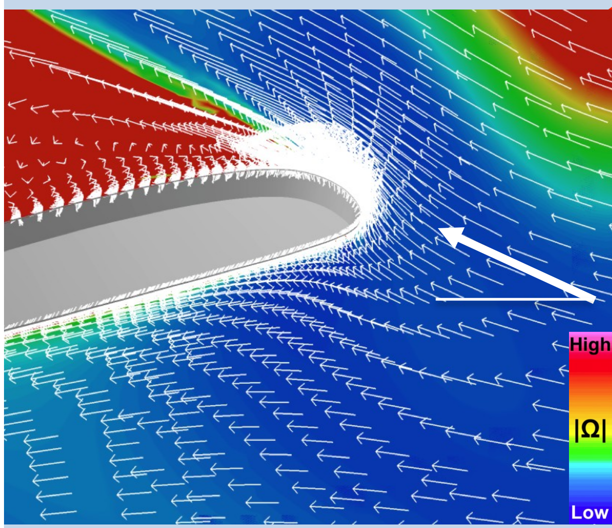

- Outboard incidence is greater than inboard incidence by at least 10 deg
- This explains why stall occurs outboard of the vortex and reattaches inboard of the vortex

Inboard of Vortex

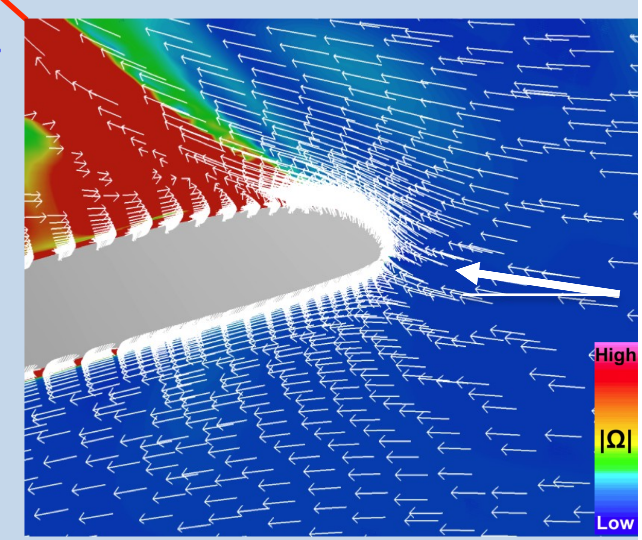

Closeup View of a Single Blade

(Same Blade Motion and Aeroelastic Deflections)

- No outboard separation in the 3rd quadrant!
    - **This confirms vortex-induced dynamic stall**
- Inboard separation due to freestream reversed flow
- Separation along entire blade in 4th quadrant, due to blade incidence

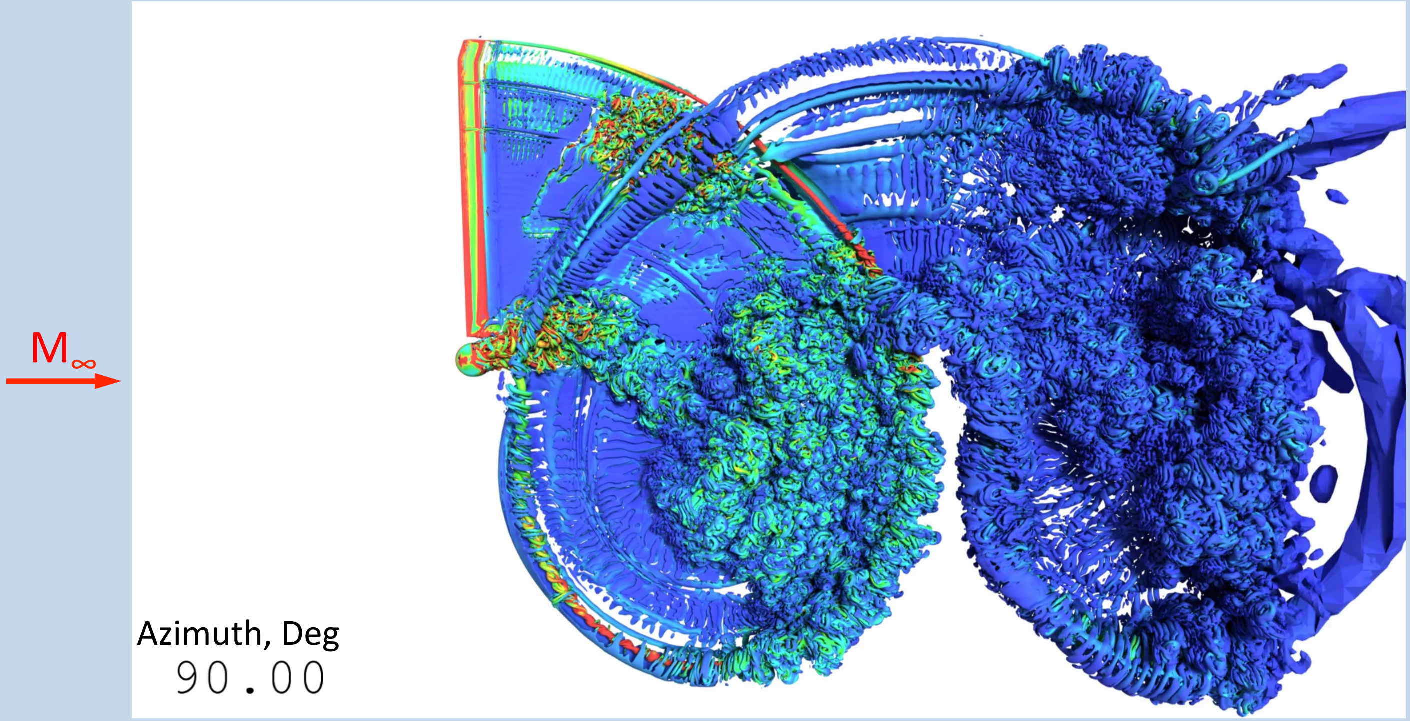

BVI-Induced Dynamic Stall (C9017)

- **First observed experimentally for a 2D airfoil**
  - 38th European Rotorcraft Forum: Zanotti, Gilbertini and Mencarelli
  - Similar explanation of how a vortex triggers dynamic stall

2D Wind-Tunnel Experiment

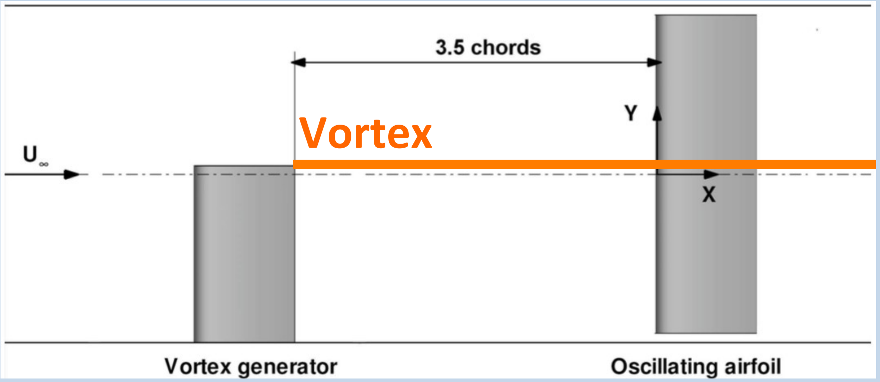

First time observed for an actual helicopter rotor

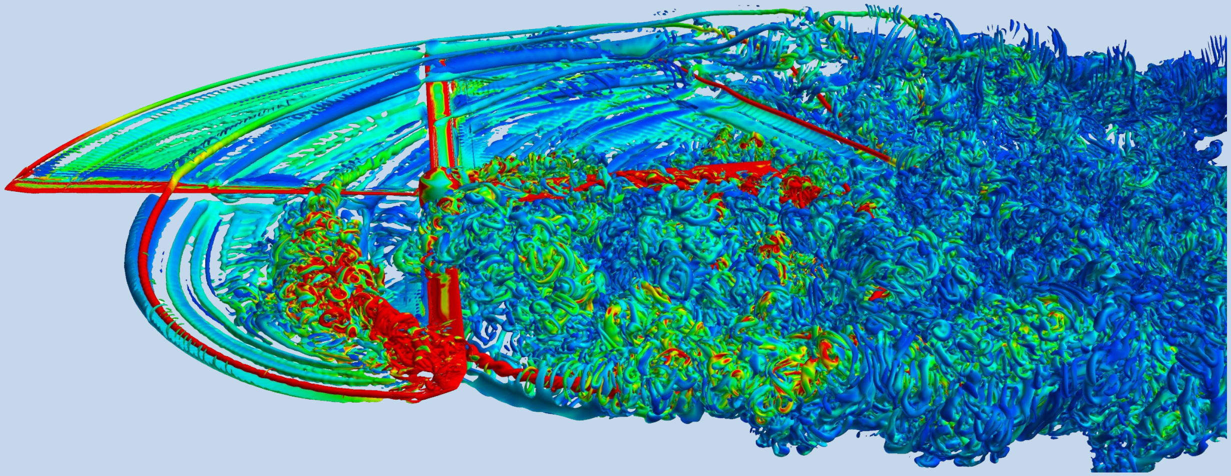

Comparison of CFD With Qualitative Flight-Test Analysis

(Dynamic Stall, C9017)

- Polar plot
  - Bousman's **moment stall**, **lift stall**, and **trailing-edge separation**
  - There are two stall events
  - CFD Outboard and inboard vortices
    - Outboard vortex initially moves inboard then outboard
  - Tracks stall closely up to 270°, where it drops below the blade and has little influence
  - Inboard vortex only moves inboard
- Flight test does not indicate inboard reversed flow
  - It must be there, but loads are light and pressure data sparse (Bousman)

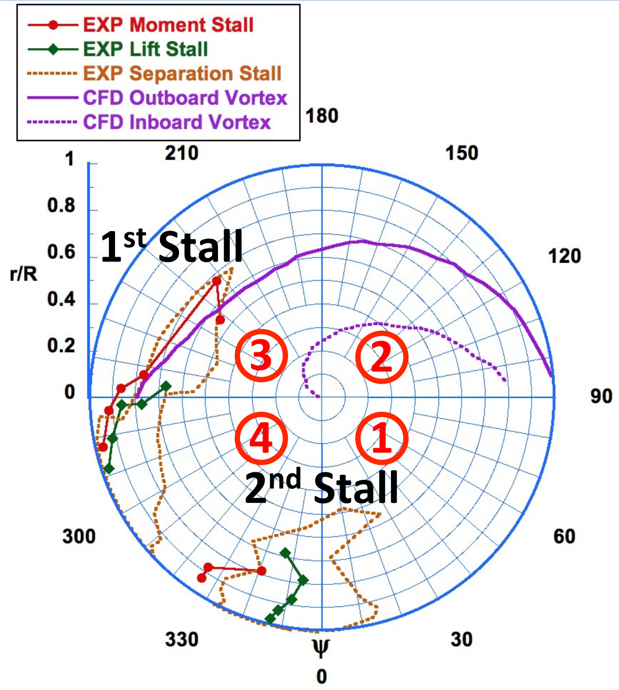

Time-Dependent Flow Visualization of Dynamic Stall Blackhawk Helicopter Rotor in Forward Flight

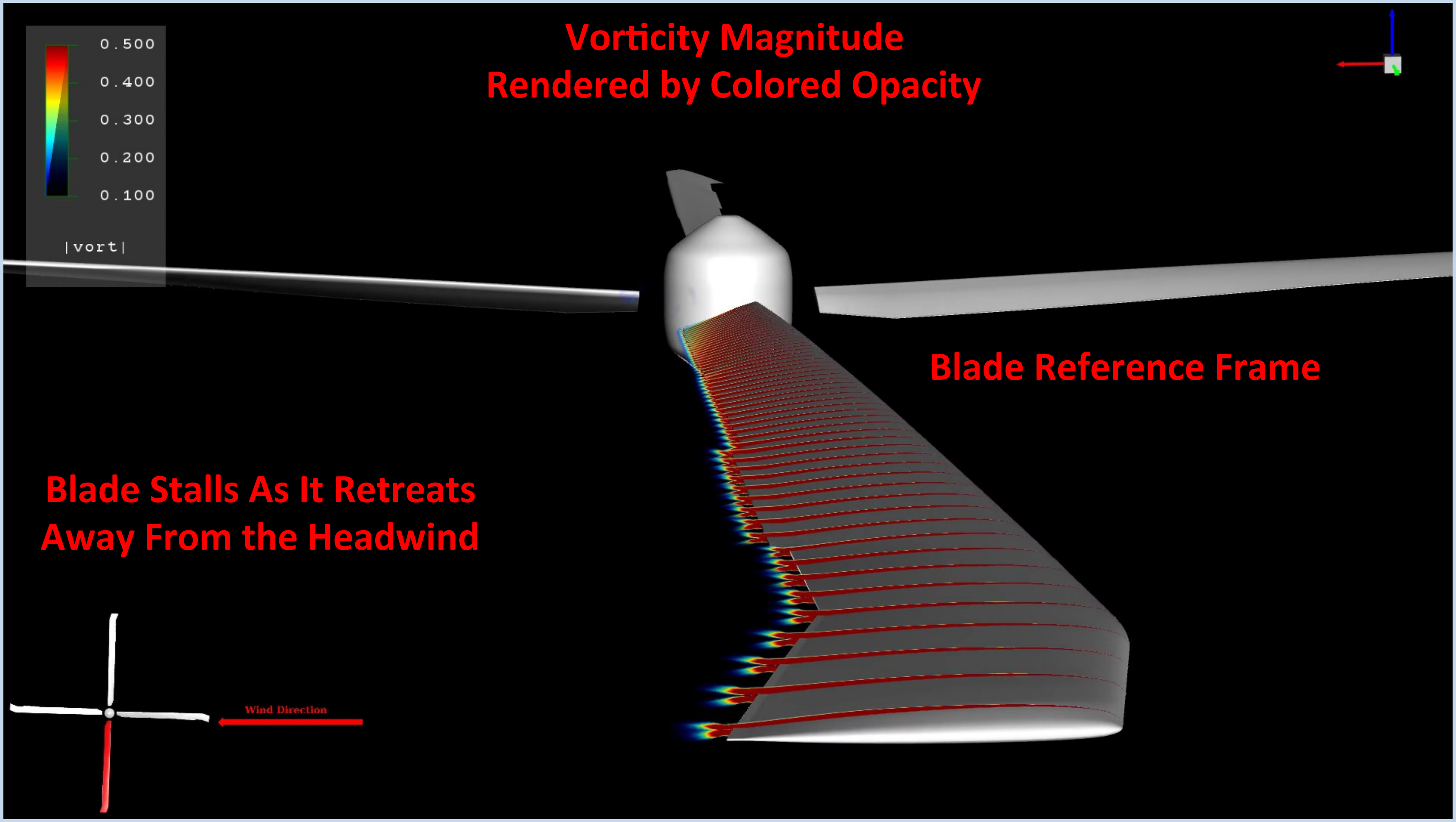

RVLT

Conclusions

- Good overall comparison between CFD airloads and flight-test measurements for BVI and dynamic stall cases
  - wake grid resolutions were ΔS=10%, 5%, and 2.5% C_{tip}
- Refining rotor wakes beyond engineering resolution (ΔS=10% C_{tip}) did not significantly affect the predicted airloads, even with blade/wake interaction
  - ❖ This suggests that airloads engineers may use the coarser wake-grid resolution (ΔS=10%c_{tip}) for hover and forward fight simulations provided
    - The CFD tip-vortex is accurately formed using a combination of fine surface mesh at the blade tip and high-order spatial accuracy
    - Use of a hybrid RANS/DDES turbulence model

Conclusions
(Continued)

- Differences between 2D and 3D dynamic stall
  - 3D vortex rings are emitted rather than a simple 2D leading-edge vortex
  - Dynamic stall flow separation can alter the path of a BVI vortex
  - Vortices passing over the rotor blade caused BVI which triggered dynamic stall
    - This phenomenon has been observed in a 2D wind-tunnel experiment
  - Mechanism for BVI-triggered dynamic stall
    - Induced velocity field by other blade-tip vortices changed the relative angle of attack of the stalling rotor blade
      - The blade AOA increased outboard of the BVI vortex, causing flow separation
      - The blade AOA decreased inboard of the BVI vortex, resulting in attached flow
- The successful modeling of 3D dynamic stall with BVI should include an accurate prediction of blade-tip vortex trajectories

Acknowledgements

- Mr. Tim Sandstrom for truly state-of-the-art time-dependent flow visualization
- Mr. Bill Bousman for his helpful discussions of the UH-60A flight test
- NASA's RVLT Program for supporting this work
- NASA's Advanced Supercomputing (NAS) Division (Pleiades Supercomputer)